

## Clusters in Polymer–Surfactant AOT Microemulsions Probed by Excited State Quenching Kinetics

Pedro M. R. Paulo, César A. T. Laia, and Sílvia M. B. Costa\*

Centro de Química Estrutural, Complexo 1, Instituto Superior Técnico, Av. Rovisco Pais 1, 1049-001 Lisboa, Portugal

Received: September 10, 2002

Excited-state quenching kinetics were applied to sodium 1,4-bis(2-ethylhexyl)sulfosuccinate (AOT) reversed micelles with poly(oxy)ethylene (POE) of molecular weight 35 000 Da where clusters were previously detected [Laia, C. A. T.; Brown, W.; Almgren, M.; Costa, S. M. B. *Langmuir* **2000**, *16*, 465]. The data obtained in AOT reversed micelles, with a fixed value of the molar ratio of water to surfactant ( $w_0 = [\text{H}_2\text{O}]/[\text{AOT}]$ )  $w_0 = 20$ , were compared in the absence and presence of the polymer. Two reaction time scales were investigated with different probes: 1,3,6,8-pyrenetetrakisulfonic acid (PTSA) in the nanosecond range and  $\text{Cr}(\text{bpy})_3^{3+}$  in the microsecond range, using, respectively, time-resolved fluorescence with picosecond resolution and laser flash photolysis techniques. The experimental decays were analyzed assuming two components, one due to polymer-free micelles described by a Poisson distribution model kinetics and another associated with the polymer-induced micelle clusters, analyzed according to a model based on the concept of random walks in regular compact lattices. A step frequency,  $k_w = 10^7 \text{ s}^{-1}$ , was extracted from the nanosecond results for the quencher's random walk within the cluster. By contrast, the triplet absorption quenching studies did not distinguish between free micelles and clusters and afforded an aggregation number for the former in the range  $260 \pm 40$ , in good agreement with literature data. Decay simulations confirm the validity of the data treatment used in the nanosecond range, but the short time behavior predicted in the microsecond range was not observed within the equipment time resolution.

### Introduction

The structural and dynamic properties of microemulsions were thoroughly studied by different techniques and are now fairly understood.<sup>1–10</sup> These systems are composed by two immiscible components stabilized by surfactants and present very rich phase behavior. In the case of water-in-oil (w/o) sodium 1,4-bis(2-ethylhexyl)sulfosuccinate (AOT) microemulsions, the aqueous pseudophase is dispersed in the oil continuous phase, with the AOT localized at the interface having the polar sulfosuccinate group oriented into the water domain and the apolar aliphatic tails turned outward. A single-phase region comprising spherical water droplets covered by a surfactant monolayer occurs in these microemulsions over a wide range of temperature and composition. The similarities between these molecular organizations and biological structures, such as the interior of cell membranes, have motivated the investigation of these systems.<sup>11</sup> In this context the inclusion of large molecules, such as proteins<sup>12–14</sup> and polymers,<sup>15–17</sup> is of particular interest and a better understanding of the effects involved could contribute to the future development and design of practical applications in such areas as drug delivery, synthesis in nano-confined media, chemical separation processes, and bio-mimetic systems.<sup>11,18–20</sup>

Polymer–surfactant systems consisting of AOT in isooctane with the water-soluble polymer poly(oxy)ethylene (POE) form microemulsions which have already been the subject of a previous dynamic and static light scattering study.<sup>21</sup> Their structure was found to depend significantly on the water pool and polymer relative sizes. If the polymer fits inside the water

pool, then the structure of these microemulsions is not greatly affected and the micellar aggregates retain their spherical shape with the polymer chain being completely encapsulated. In this case, an increase in AOT superficial area and on the interfacial elastic modulus of the surfactant monolayer was noticed due to the adsorption of the polymer in the interfacial region.<sup>21–24</sup>

On the other hand, when the polymer does not fit inside a single water droplet a bead necklace type of structure was proposed, with the polymer chain serving as the backbone to a cluster of reversed micelles.<sup>16,22</sup> The size of these structures is practically independent of the volume fraction of the dispersed phase as these are nonpercolating systems. The driving force for the cluster formation is the solubilization of the polymer in the aqueous domain rather than the increase of attractive forces between micelles that occurs, in AOT w/o microemulsions, when the temperature or the dispersed phase volume fraction is increased. Light scattering results indicate that the aggregates' population is essentially bimodal in these microemulsions and composed of polymer-induced clusters and free reversed micelles, the latter similar to those found in AOT microemulsions without polymer.<sup>21</sup>

Clustering phenomena in microemulsions has been studied by several methods such as nonradiative energy transfer,<sup>25</sup> triplet–triplet annihilation,<sup>26</sup> conductivity and dielectric measurements,<sup>27–30</sup> Kerr effect and viscosity measurements,<sup>31</sup> light scattering techniques,<sup>32,33</sup> and steady-state fluorescence quenching.<sup>9</sup> Almgren and co-workers studied AOT w/o microemulsions in the cluster regime of the  $L_2$  phase using time-resolved luminescence quenching with fluorescent and phosphorescent probes to survey different time scales.<sup>34–36</sup> These authors

\* Corresponding author. E-mail: sbcosta@popsrv.ist.utl.pt.

developed several models to describe the quenching phenomena in these media considering the cluster structure and/or quencher occupancy number. A model based on the concept of random walk in regular lattices was adapted for percolating clusters with either a compact or an open and ramified structure, while for clusters of small dimensions a modification of the Infelta-Tachiya quenching kinetics model<sup>37,38</sup> in micellar media was presented.

The aim of the present work was to obtain dynamic information on polymer-induced clusters formed in AOT microemulsions that could further elucidate the structure of these aggregates. For this purpose, AOT microemulsions with  $w_0 \equiv [\text{H}_2\text{O}]/[\text{AOT}] = 20$  and POE of molecular weight 35 000 Da were selected since the light-scattering results point to a population dominated by polymer-induced clusters.<sup>21</sup> The excited-state quenching kinetics of two probes—a short-lived, 1,3,6,8-pyrenetetrasulfonic acid (PTSA), and a long-lived, tris-(2,2'-bipyridine)chromium(III) ( $\text{Cr}(\text{bpy})_3^{3+}$ )—by the same quencher  $\text{I}^-$ , incorporated in these microemulsions, were used as a means to test the applicability of an additive kinetic model to the nonpercolative clusters detected herein. In the absence of intermicellar exchange of solutes, these systems can be treated in terms of two different structural models associated, respectively, to the small polymer-free micelles and large compact polymer-induced clusters.

## Theory

Infelta<sup>37</sup> and Tachiya<sup>38</sup> pioneered the modeling for the quenching kinetics of an excited probe by a diffusing species in micellar media and obtained the following expression for the dependence of the probe signal intensity with time:

$$I(t) = A_1 \exp[-A_2 t - A_3(1 - \exp(-A_4 t))] \quad (1)$$

The  $A_1 - A_4$  parameters appearing in eq 1 have the following meaning:

$$A_1 = I(0) \quad (2)$$

$$A_2 = k_0 + \frac{k_q k_e}{k_q + k_e [\text{M}]} [\text{Q}]_t \quad (3)$$

$$A_3 = \left( \frac{k_q}{k_q + k_e [\text{M}]} \right)^2 n \quad (4)$$

$$A_4 = k_q + k_e [\text{M}] \quad (5)$$

where  $I(0)$  is the probe intensity signal at time  $t = 0$ ,  $k_0$  is the probe natural excited-state decay rate constant,  $k_q$  is the pseudo-first-order intramicellar quenching rate constant,  $k_e$  is the intermicellar rate constant for the exchange of solutes, and  $n$  is the average occupation number of the quencher species in the micellar media, which can be related to the average aggregation number of surfactant molecules,  $N_{\text{agg}}$ , that compose a micelle:

$$n = \frac{[\text{Q}]_t}{[\text{M}]} = \frac{[\text{Q}]_t}{[\text{S}] - C_{\text{c.m.c.}}} N_{\text{agg}} \quad (6)$$

This expression assumes that the population of aggregates is monodisperse and that the distribution of solutes among these follows the Poisson distribution law. It further assumes that the exchange process occurs through a fusion–fission mechanism, with coalescence of the water pools for reverse micelles. In the case of short-lived probes, the exchange process may be

insignificant during the lifetime of the probe, in which case expression (1) simplifies to

$$I(t) = I(0) \exp[-k_0 t - n(1 - \exp(-k_q t))] \quad (7)$$

Almgren and co-workers developed a similar expression for the situation of reversed micelles aggregation in clusters:<sup>34,35</sup>

$$I(t) = I(0) \exp[-k_0 t - n(1 - \exp(-k_q t)) - (n_c - n)(1 - \exp(-k_{\text{cq}} t))] \quad (8)$$

where  $n_c$  is the average occupation number of quencher molecules per cluster and it can also be formulated as  $n_c = m \times n$ , with  $m$  as the average number of micelles per cluster. The parameter  $k_{\text{cq}}$  refers to the rate constant for intracuster quenching, which can be perceived as the product of the jump frequency of the quencher over the micelles in the same cluster by the probability of finding an excited probe in the next jump. The other constants retain the same meaning as before. Expression (8) is valid for monodisperse clusters of relatively small size and composed of micelles of the same structure as the free micelles in solution. This is the situation of AOT microemulsions below the percolation threshold, in which the clustering phenomena results from an increase in the attractive forces between micelles. Any polydispersity effects in the average aggregation number,  $N_{\text{agg}}$ , or in the average number of micelles per cluster,  $m$ , can be dealt with, a posteriori, following the treatment introduced by the same authors.<sup>34,39</sup>

The modified Infelta-Tachiya model no longer holds for large clusters and the following model is more appropriate to describe the quenching kinetics:

$$I(t) = I(0) \exp[-nS(k_w t)] \exp(-k_0 t) \quad (9)$$

with

$$S(k_w t) = \begin{cases} a_1 (k_w t)^{d_s/2}, & d_s < 2 \\ a_2 (k_w t), & d_s > 2 \end{cases} \quad (10)$$

where  $k_w$  is the step frequency,  $a_1$  and  $a_2$  are constants,  $d_s$  is the spectral dimension of the domain, and the other constants have the same meaning as before. For clusters in the percolating region it is expected, from the Alexander and Orbach conjecture, that  $d_s = 4/3$  and the quenching process should exhibit a fractal behavior. On the other hand for large compact clusters, such as the ones formed well above the percolation threshold,  $d_s > 2$  is verified and an exponential decay is predicted for the excited probe.

## Experimental Section

**Materials.** Sodium 1,4-bis(2-ethylhexyl)sulfosuccinate (AOT) was purchased from Sigma and used as received. The isooctane was also from Sigma-Aldrich with HPLC grade. Poly(oxy)-ethylene was purchased from Fluka and used without further purification. The polymer polydispersity  $M_w/M_n$  ranges were between 1.1 and 1.2. The water employed in the samples' preparation was double distilled. Sodium pyrenetetrasulfonate (PTSA) from Molecular Probes was used as received. Potassium iodide with 99% purity was supplied by Aldrich. Tris(2,2'-bipyridine)chromium(III) ( $\text{Cr}(\text{bpy})_3^{3+}$ ) was a kind gift from Professor Mauro Maestri of Bologna University.

The microemulsions were prepared by successive additions of adequate volumes from aqueous concentrated solutions of the different components to a 0.1 M AOT stock solution in isooctane. Sometimes complete solubilization required inter-

mediate steps of agitation between the components addition and heating of the samples until visual clarity was achieved. The water content used was fixed ( $w_0 = 20$ ) and the polymer concentration was kept at 1% (w/w) in the aqueous phase, except when stated otherwise. The probe concentrations used were  $5 \times 10^{-6}$  M for PTSA and  $2 \times 10^{-5}$  M for  $\text{Cr}(\text{bpy})_3^{3+}$ . Whenever required, the samples were degassed by bubbling with a stream of high-quality argon saturated in isooctane.

**Apparatus.** Absorption spectra were recorded in a Jasco V-560 UV–vis spectrophotometer, while steady-state emission spectra were measured with a Perkin-Elmer LS 50B spectrofluorimeter.

Fluorescence decays were obtained from time-correlated single-photon counting technique (SPC) with picosecond resolution, using a Coherent Innova 400-10 argon ion laser to synchronously pump a Coherent 701-2 (DCM) dye laser.<sup>40</sup> The decays were acquired with sample excitation at 335 nm and detection at 385 nm, with 20 000 counts in the maximum channel. Data analysis was performed with software provided by Photon Technology International and with a program developed at the laboratory. In both cases, the decays are fitted to the model expressions by using a nonlinear least-squares method based on the Marquardt algorithm<sup>41</sup> combined with an iterative reconvolution procedure to account for the distortion introduced by the instrumental response function (IRF).<sup>42</sup> The quality of the results was judged by the usual statistical criteria, analyzing the values of  $\chi^2$  (0.9–1.2), DW (1.7–1.8), and the distribution of residuals and autocorrelation functions.

Transient absorption measurements were performed with laser flash photolysis equipment previously described.<sup>43</sup> The third harmonic (355 nm) of an Nd:YAG Quanta-Ray GCR-3 Spectra-Physics laser was used as the excitation source, while detection was carried at 400 nm, in a 90° arrangement, using a Xe lamp as the probe signal. The samples were also thermostated at 25 °C. For each decay an average of 8 to 32 curves were accumulated and analysis was performed with a nonlinear least-squares method using commercial software.

## Results and Data Analysis

**i. Fluorescence Quenching.** In the nanosecond time scale, the pair PTSA/I<sup>−</sup> was employed in the time-resolved fluorescence quenching experiments (TRFQ). This probe has a natural lifetime around 11 ns in the singlet excited state in water and it allows spanning a time window of about 40 ns—see Figure 1.

A previous study in aqueous solution of POE was carried out to assess the effect of this polymer on the time-resolved fluorescence behavior of PTSA. The decays obtained were biexponential for the range of polymer concentrations surveyed (1–10 wt %). A global analysis was performed with two common lifetimes and satisfactory fits were achieved for all decays. This procedure yielded two lifetimes of 11.3 and 8.82 ns, with the higher of these values corresponding to the probe's natural lifetime in water (PTSA<sub>w</sub>). The other lifetime was attributed to the PTSA adsorbed onto the polymer (PTSA<sub>a</sub>) and as expected the preexponential,  $F_2$ , associated with this component increases with polymer concentration—Table 1. The variation of the  $F_2$  normalized values was modeled with a two-state model according to Scheme 1. Each polymer chain is assumed to provide an average number of “sites” where the adsorption of the probe can occur and the overall concentration of “sites” is taken to be proportional to the concentration of polymer. Besides that, it is also assumed that during the lifetime of the excited probe the conversion between the aqueous and

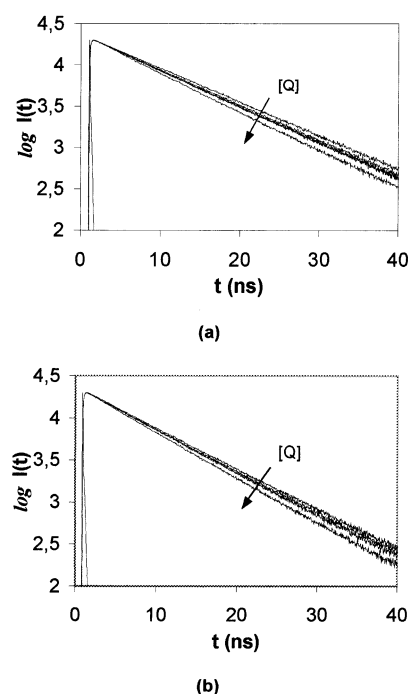


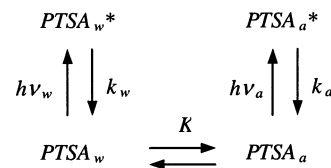
**Figure 1.** Fluorescence decays of PTSA in AOT microemulsions ( $w_0 = 20$ ) obtained by SPC technique: (a) without polymer (quencher concentrations  $[Q] = 0, 0.050, 0.075, 0.100$  and  $0.200$  mM) and (b) with POE MW35,000 1 w % ( $[Q] = 0, 0.050, 0.100$  and  $0.200$  mM).

**TABLE 1: Absorption and Emission Maxima and Decay Analysis Parameters for PTSA in Aqueous Solution of POE**

POE (wt %)	$\lambda_{\text{abs}}^{\text{max } a}$ (nm)	$\lambda_{\text{fl}}^{\text{max } b}$ (nm)	$F_2^c$	$\chi^2^d$	D.W. <sup>e</sup>
0	374.5	385	0	1.169	1.844
0.5	374	385.5			
1	374.5	385	0.212	1.205	1.961
2	374	384.5	0.349	1.151	1.794
3	374	384.5			
4	374.5	384	0.518	1.253	1.788
5	374.5	385	0.600	1.239	1.764
10	375	384.5	0.804	1.244	1.649

<sup>a</sup> Wavelength of absorption maximum. <sup>b</sup> Wavelength of emission maximum. <sup>c</sup> Preexponential of the short lifetime component. A global analysis afforded two lifetimes of 11.3 and 8.82 ns for the SPC decays. <sup>d</sup> Chi-square for biexponential fits of fluorescence decays. <sup>e</sup> Durbin-Watson for biexponential fits of fluorescence decays.

### SCHEME 1



the adsorbed form is negligible, so that the preexponentials obtained from the decays reflect the balance of these two populations in the ground state. Although this is a very simple model, it explains the experimental data reasonably well. Nevertheless, a different nature for the interaction between the POE and PTSA could be argued, where the existence of several solubilization sites for the probe in the polymer solution leads to a distribution of lifetimes that globally would be revealed as a biexponential decay.

*i.a. AOT Microemulsions without Polymer.* The first system to be studied was the AOT microemulsion with  $w_0 = 20$  and without polymer to compare with the known literature data. The decays obtained were fitted with expression (1) and the

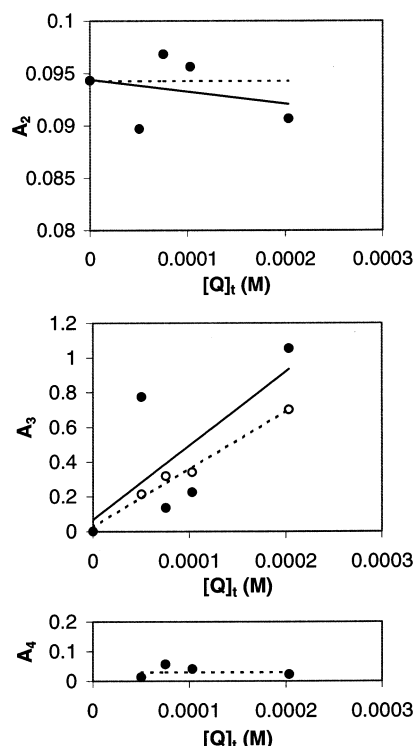


**Figure 2.** Values of the  $A_2$ ,  $A_3$ , and  $A_4$  parameters adjusted for the PTSA decays in AOT microemulsion without polymer ( $w_0 = 20$ ) from individual fitting of decays (closed circles and full lines) and from global analysis considering  $A_2$  and  $A_4$  as common parameters (open circles and dashed lines).

**TABLE 2: Values of the Rate Constants  $k_0$ ,  $k_q$ , and of the Average Aggregation Number,  $N_{agg}$ , for AOT Microemulsion without Polymer ( $w_0 = 20$ ), Obtained from Fluorescence Quenching of PTSA with  $I^-$**

$k_0$ ( $10^7$ s $^{-1}$ )	9.43
$k_q$ ( $10^7$ s $^{-1}$ )	2.98
$N_{agg}$	333

variations of the  $A_2$ ,  $A_3$ , and  $A_4$  parameters with the quencher concentration are presented in Figure 2. A linear relation between  $A_2$  and the quencher concentration that could evidence intermicellar exchange processes was not found. This is not surprising if one considers the probe's short lifetime.<sup>39</sup> So the results were interpreted according to expression (7), assuming that no significant solute exchange occurs within the lifetime of the excited probe. The same decays were again analyzed considering  $A_2$  and  $A_4$  as global parameters, and a significant improvement was achieved in the linear relation of  $A_3$  with quencher concentration without compromising the quality of the individual decay fittings (see Figure 2). The rate constants  $k_0$  and  $k_q$  obtained along with the average aggregation number,  $N_{agg}$ , are presented in Table 2.

From the graphical representation of the decays obtained (Figure 1a), it is not possible to observe the typical nonexponential deviation predicted by Infelta-Tachiya expression at short times. This results from the balance of the constants  $A_2$  and  $A_4$ , and these in turn are determined by the intrinsic characteristics of the system studied along with the properties of pair probe/quencher used. From computer-generated curves with expression (1), it was assessed that the ratio  $A_4/A_2$  should be higher than 1 in order to obtain a well-developed decay.<sup>44</sup> In the present work, this ratio is about 0.5 and therefore it is difficult for the fitting algorithm to discern between a set of solutions in which higher values of  $A_2$  and  $A_4$  are compensated by a somewhat lower  $A_3$ . This leads to a systematic error in the fitting procedure which

## SCHEME 2

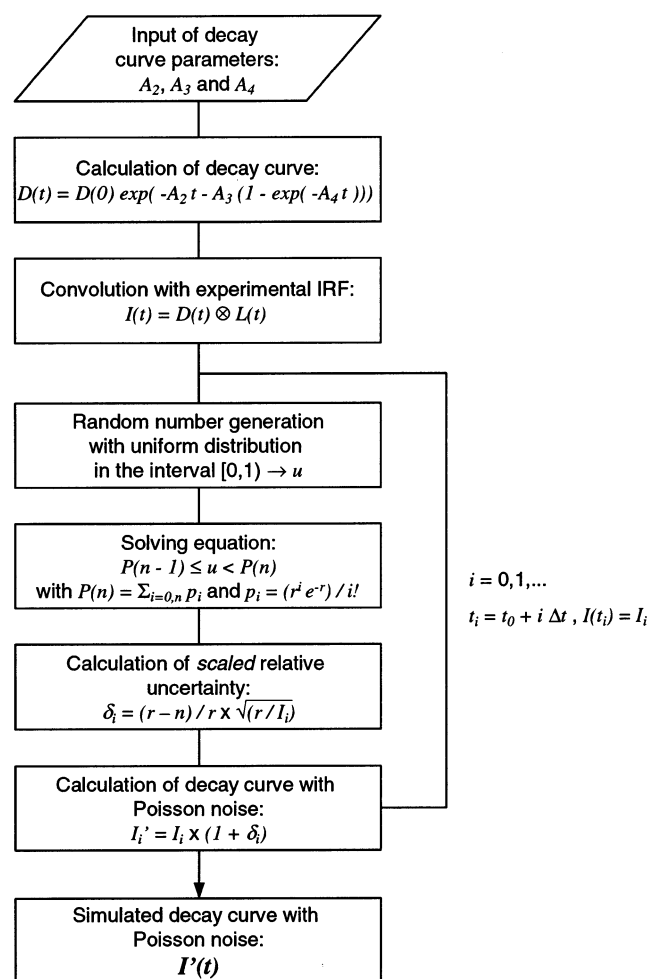


**TABLE 3: Values of the Constants  $k_0$ ,  $k_q$ ,  $k_e$ , and  $N_{agg}$  Used to Simulate a Set of Decays (Sim. 1 and 2, See Text for Further Details) and of the Same Constants for the Fitted Curves with Expressions (1) to (5) – Fit 1 – and with Expression (7) – Fit 2**

	sim. 1	sim. 2 <sup>a</sup>	fit 1	fit 2
$k_0$ ( $10^7$ s $^{-1}$ )	9.43	9.17	9.42	9.17
$k_q$ ( $10^7$ s $^{-1}$ )	5.00	5.00	4.97	4.08
$k_e$ ( $10^{10}$ M $^{-1}$ s $^{-1}$ )		2.10	0.49	
$N_{agg}$	285	283	273	321

<sup>a</sup> Values taken from ref 46.

then shows as a pseudolinear dependence of  $A_2$  on  $[Q]_t$ , that could be interpreted as an evidence of intermicellar exchange processes. The uncertainties introduced by the Poisson noise characteristic of SPC curves further aggravate this deviation. This scenario was confirmed using computational simulation of SPC decay curves. To ensure that the simulation conditions were as close to reality as possible, besides convoluting the calculated decay curves with the instrumental response function of the SPC apparatus, characteristic Poisson noise was also introduced through a Monte Carlo simulation routine as presented in Scheme 2.

For the purpose of evaluating the quality of the fitting results, two sets of decays were simulated, with and without the input of  $k_e$ , using typical values for the parameters in expression (1)—see Table 3. In the latter case,  $A_2$  and  $A_4$  were taken as common parameters with the values given in Figure 3 by the horizontal lines and  $A_3$  values were calculated from expression (6)



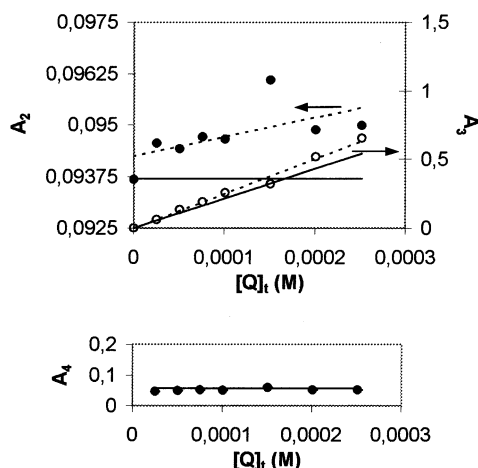


**Figure 3.** Values of the  $A_2$ ,  $A_3$ , and  $A_4$  parameters used in the simulation of a set of decays (full lines) and for the same curves fitted with expression (1) (open and closed circles; dashed lines).

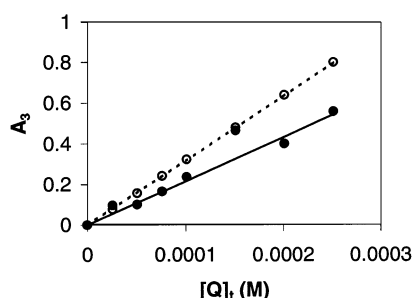


**Figure 4.** Values of the  $A_3$  used in the simulation of a set of decays (full line) and for the same curves fitted with expression (1) and (7)—closed and open circles, respectively, for the micellar quenching kinetics with and without intermicellar solute exchange.

assuming  $N_{\text{agg}} = 285$ . The simulated decays obtained were then fitted with the analysis program considering  $A_2$  and  $A_4$  as independent parameters, and the values adjusted are presented in Figure 3 as the function of the quencher concentration assumed. The systematic deviation of the  $A_2$  parameter to values higher than the simulation input values could be mistaken with the linear variation vs the quencher concentration predicted for intermicellar exchange of solutes, and expressions (2)–(5) could then be used to interpret the fitted data. The results for the set of constants  $k_0$ ,  $k_q$ ,  $k_e$ , and  $N_{\text{agg}}$  obtained in this way are presented in Table 3 (fit 1). The values resemble the ones used in simulation, but the  $k_e$  obtained in the order of  $10^9$ – $10^{10}$   $\text{M}^{-1} \text{s}^{-1}$  results merely from the difficulty of the fitting algorithm to produce accurate values for the  $A_2$  parameter. In the other simulation, the opposite approach was tested by adjusting simulated decays with a nonzero  $k_e$  value using expression (7). The curves were well fitted with both equations—see Table 3 (fit 2) and Figure 4—showing that for this spread of  $A_2$ – $A_4$  values it is not possible to extract exchange rate constants with physical significance using this method.

*i.b. AOT Microemulsions with POE MW35 000.* As already mentioned, a bimodal population of aggregates containing polymer-induced clusters and free reversed micelles is present in the polymer–surfactant microemulsions studied in this work. The kinetics of the quenching process in such a system can be modeled with a weighted law for the two populations involved, considering a fraction  $\alpha$  that accounts for the amount of signal proceeding from the clusters.

$$\frac{I(t)}{I(0)} = (1 - \alpha) \exp[-k_0 t - n(1 - \exp(-k_q t))] + \alpha I_C(t) \quad (11)$$

The first term in the right-hand side of expression (11) describes the quenching kinetics in the population of free reversed micelles and corresponds to the Infelta-Tachiya expression simplified for negligible intermicellar exchange of solutes. The  $I_C$  term refers to the quenching processes in the polymer-induced clusters and, assuming that the models developed for the percolative type of clusters are applicable, expressions (8) or (9) can be used, respectively, for small aggregates and large ones with either a compact or an open and ramified structure. This simplistic treatment requires that, within the lifetime of the probe, the only significant exchange processes should occur between the micelles of the same cluster.

A similar approach was proposed to model the fluorescence decay kinetics of mixed micelles and vesicles systems,<sup>45</sup> but the large number of parameters to be fitted compromised its applicability.

When expression (11) is applied to the nanosecond time scale along with expression (8) for the  $I_C$  term, a further simplification is possible given the discrepancy in the order of magnitude of the quenching rate constants involved—usually  $k_q, k'_q \gg k_{cq}$ . In the short time domain, the exponential involving  $k_{cq}$  in the second term of expression (8) can be approximated by the first two terms in the series expansion:

$$\exp(-k_{cq} t) \approx 1 - k_{cq} t \quad (12)$$

from which it results:

$$\left( \frac{I(t)}{I(0)} \right)_{\text{st}} = (1 - \alpha) \exp[-k_0 t - n(1 - \exp(-k_q t))] + \alpha \exp[-(k'_0 + n'(m - 1)k_{cq})t - n'(1 - \exp(-k'_q t))] \quad (13)$$

The prime quantities appearing in the second term have the same meaning as before, but refer to the cluster population.

The decays obtained for PTSA in the microemulsions with POE MW35 000—see Figure 1b—were initially fitted with expression (13). The set of parameters appearing in the first term were fixed at the values previously found for the microemulsions without polymer. This corresponds to considering that the structure of the free reversed micelles (not in clusters) is not perturbed by the presence of the polymer, which seems a reasonable approximation given the stability of the micellar aggregates in AOT microemulsions.<sup>36,39</sup> In this way the adjustable parameters were reduced to those concerning the fraction of signal attributed to the population of reversed micelles in polymer-induced clusters:  $\alpha, k'_0, n', k'_q$  and  $n'(m - 1)k_{cq}$ —fitted as a single parameter. A different value for the natural decay rate constant was allowed for the probe located in the clusters, since the decay curve in the absence of quencher is not single exponential. Following this procedure it was possible to obtain good fits for the decays; however, in all cases the parameter  $k'_q$  converged to negligible values, indicating that the term  $n'(1 - \exp(-k'_q t))$  has no significance in the description of the decay curves. In practice, the difference between the decay profiles for the microemulsions without and with polymer could be accounted for simply by an additional single exponential with a weight of about 70–80%.

This situation is better described by the model presented for large clusters with a compact structure, which corresponds to

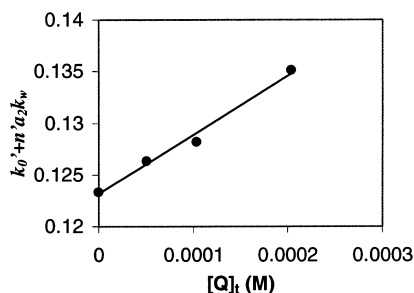


**Figure 5.** Values of the second exponential component fitted for the PTSA decays in AOT microemulsion with POE MW35 000 ( $w_0 = 20$ ) using expression (14).

**TABLE 4: Values of the Parameter  $\alpha$  and of the Constants  $k_0'$  and  $a_2k_w/[M]'$  for AOT Microemulsion with POE MW35 000 ( $w_0 = 20$ ), Obtained from Fluorescence Quenching of PTSA with  $I^-$**

$\alpha$	0.71
$k_0' (10^7 \text{ s}^{-1})$	12.32
$a_2k_w/[M]' (10^{10} \text{ M}^{-1} \text{ s}^{-1})$	5.71

use of expression (9) for the  $I_C$  term of expression (11), with  $k_w$  defined for the condition  $d_s > 2$ .

$$\left(\frac{I(t)}{I(0)}\right)_{\text{st}} = (1 - \alpha) \exp[-k_0 t - n(1 - \exp(-k_q t))] + \alpha \exp[-(k_0' + n'a_2k_w)t] \quad (14)$$

In this case, the set of constants  $a_2k_w/[M]'$  can be determined from the slope of the linear dependence of the second exponential component with quencher concentration—see Figure 5—and  $k_0'$  from its origin. The values obtained for these constants along with the fitted  $\alpha$  parameter are presented in Table 4. The natural decay rate constant retrieved for the probe located in the polymer-induced clusters,  $k_0'$ , corresponds to a lifetime of 8.12 ns which compares well with the lifetime attributed to PTSA adsorbed on POE. This supports the bimodal interpretation of the decay components regarding the population of the probes in the micellar aggregates that compose these microemulsions.

**ii. Transient Absorption.** In the experiments in the microsecond time domain, the pair  $\text{Cr}(\text{bpy})_3^{3+}/I^-$  was employed and the primary transient absorption of the probe was followed by the optical density difference using laser flash photolysis.

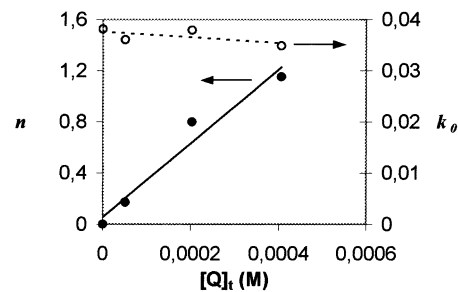
*ii.a. AOT Microemulsions without Polymer.* The decays obtained were single exponential, but a decrease in the initial intensity of the signal was noticed with the increase in quencher concentration. The Infelta-Tachiya model was used to interpret these results considering that in the microsecond time scale the term  $\exp(-k_q t)$  is negligible. Furthermore, assuming that  $k_q \gg k_0$  and  $k_e[M]$  for the pair probe/quencher used expression (1) is simplified to

$$I(t) = I(0) \exp[-(k_0 + k_e[Q])t - n] \quad (15)$$

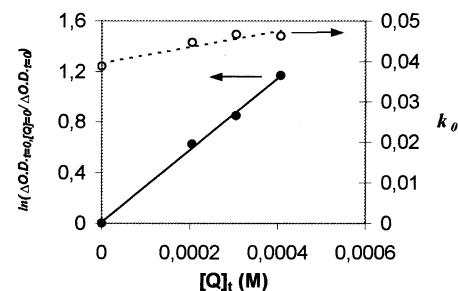
which describes well the behavior observed for the decays obtained. Accordingly, from the initial jump in the signal intensity of the decays it is possible to retrieve an average aggregation number for the micelles that compose this microemulsion—see Table 5—that agrees well with the values reported in the literature and within experimental error with the  $N_{\text{agg}}$  extracted from TRFQ. It was not possible to ascertain if intermicellar exchange of solutes is significant during the lifetime of the excited probe from the slope of the logarithmic plot of the decays—see Figure 6a—given the noise these curves

**TABLE 5: Values of the  $\text{Cr}(\text{bpy})_3^{3+}$  Transient Lifetime,  $\tau_0$ , and of the Average Aggregation Number,  $N_{\text{agg}}^{\text{av}}$ , for the AOT Microemulsions Studied, Obtained from Excited State Quenching with  $I^-$**

	$\tau_0 (\mu\text{s})$	$N_{\text{agg}}^{\text{av}}$
no polymer	27	287
[POE] = 1%	25	283
[POE] = 1.5%	25	240



(a)



(b)

**Figure 6.** Values of the rate constant  $k_0$  and  $\log(\Delta O \cdot D \cdot (0)_{[Q]=0} / \Delta O \cdot D \cdot (0))$  obtained from fitting expression (17) to  $\text{Cr}(\text{bpy})_3^{3+}$  decays in AOT microemulsions ( $w_0 = 20$ ) without polymer (a) and with POE MW35000 1 wt % (b) (see text for further details).

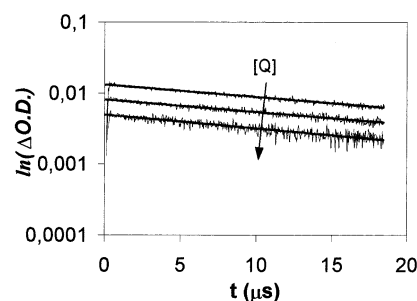
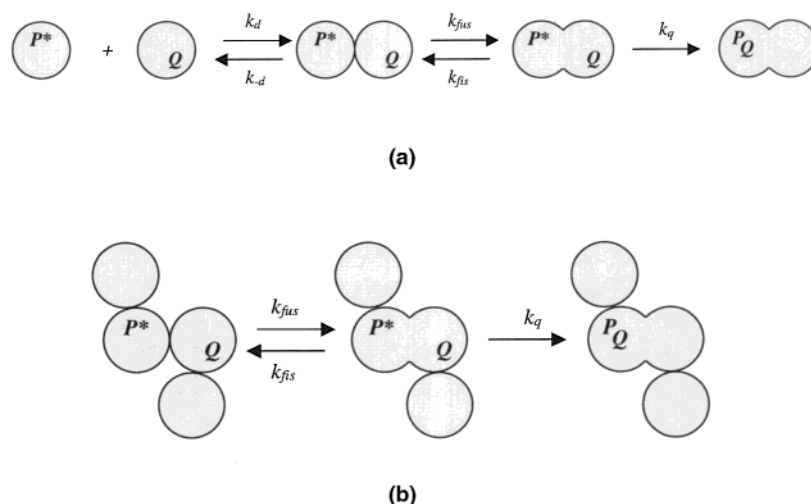


**Figure 7.** Decays obtained for  $\text{Cr}(\text{bpy})_3^{3+}$  primary transient by laser flash photolysis in AOT microemulsions ( $w_0 = 20$ ) with POE MW35,000 (1.5 wt %) ( $[Q] = 0, 0.2$  and  $0.4$  mM).

present. However an average lifetime of 27  $\mu\text{s}$  could be determined for the primary transient of  $\text{Cr}(\text{bpy})_3^{3+}$  that is in agreement with the values found by other authors.<sup>47,48</sup>

*ii.b. AOT Microemulsions with POE MW35 000.* The decay curves obtained with the AOT microemulsions using two polymer concentrations (1 and 1.5% w/w in the aqueous phase) present the same qualitative behavior as the decays of microemulsions without polymer—see Figure 7. This result can still be explained within the bimodal approach introduced in Section *i.b.*, considering some simplifications that are possible in the microsecond time scale. Beginning with the first term on the right-hand side of expression (11), this can be approximated by a single exponential with an offset as was done in the previous section—expression (15). For the  $I_C$  term concerning

## SCHEME 3



$k_d, k_{-d}, k_{fus}, k_{fiss}, k_q$  – rate constants of diffusion, dissociation, micellar fusion, micellar fission and intramolecular quenching respectively.

the cluster population, two situations must be considered. In the absence of quencher, according to expression (9) this term is a single exponential, with a decay rate constant  $k'_0$  for the excited probe located in the clusters. If this constant is similar to the probe's decay rate constant in the free reversed micelles,  $k_0$ , then a global single-exponential decay is expected:

$$\left( \frac{\Delta O \cdot D \cdot (t)}{\Delta O \cdot D \cdot (0)} \right)_{[Q]=0} = (1 - \alpha) \exp(-k_0 t) + \alpha \exp(-k'_0 t) \xrightarrow{k'_0=k_0} \exp(-k_0 t) \quad (16)$$

In the presence of quencher, the  $I_C$  term should be negligible, assuming that the set of constants  $n'a_2k_w$  is of the order of magnitude as that determined for the nanosecond TRFQ results and expression (11) is then reduced to

$$\left( \frac{\Delta O \cdot D \cdot (t)}{\Delta O \cdot D \cdot (0)} \right)_{It} = (1 - \alpha) \exp[-(k_0 + k_e[Q])t - n] + \alpha \exp[-(k'_0 + n'a_2k_w)t] \quad (17)$$

$$\approx (1 - \alpha) \exp[-(k_0 + k_e[Q])t - n] \quad (17')$$

The data treatment is therefore similar to the case of the microemulsions without polymer. From the slope of the logarithm decay plot it is possible to retrieve a decay rate constant and from the origin the initial decay intensity. These are presented in Figure 6b, using a logarithmic normalized form for the initial decay intensities in the presence of quencher, from which the set of constants  $(1 - \alpha) \exp(-n)$  can be evaluated. The results obtained are summarized in Table 5.

## Discussion

Considering the hydrophilic character of both probes and quencher used in the present work and the monodispersity of micellar aggregates in AOT microemulsions, it is reasonable to assume that the intermicellar exchange of solutes would proceed via a fusion–fission mechanism,<sup>44</sup> irrespective of these exchanges occurring between free reversed micelles or clustered ones—see schemes III (a) and (b), respectively.

In the present study, it was not possible to detect intermicellar exchange processes during the lifetime of the excited probe using TRFQ with PTSA/I<sup>−</sup> in AOT microemulsions without polymer.

Comparing the values presented in Table 2 and Table 4 for the probe's natural decay rate constant in the microemulsions studied, it is observed that a significant difference is introduced with the presence of the polymer in these systems. Poly(oxy)-ethylene is known to exhibit some affinity toward anionic species, this being the reason for its adsorption at the interface of AOT reversed micelles and very likely it interacts with PTSA, changing its singlet lifetime.

From the value adjusted for the set of constants  $a_2k_w/[M]'$ , it is possible to estimate an order of magnitude for the intermicellar random walk step frequency of the quencher in the clusters,  $k_w$ , on some basic assumptions. The  $a_2$  parameter depends on the lattice structure where the random walk takes place and, given the fact that the irregular structure of these clusters is not known, it is reasonable to assume a unit value. The micellar concentration,  $[M]'$ , can be determined considering that the aggregation number of the clustered micelles is not very different from that of free reversed micelles. This gives a  $k_w$ , around  $10^7 \text{ s}^{-1}$ , which is one to two orders of magnitude higher than the value found for percolative clusters by Almgren et al.<sup>35</sup> An increase in cluster connectivity induced by the polymer chain could be a plausible reason for this difference. The perturbation introduced by the polymer in the interfacial region of neighboring micelles in the cluster would facilitate the deformation of the surfactant monolayer from a local negative curvature to a less favorable positive curvature, thereby lowering the energy barrier associated with the fusion process. This would render higher  $k_w$  values when compared with percolating clusters of the same size. In loose terms, the polymer chain carves channels in the cluster structure that increase the communication between the water-pools of reversed micelles making the quenching process more efficient. The opposite effect cannot be excluded since it is known that the adsorption of the polymer at the interface of micellar aggregates in AOT microemulsions increases the rigidity of the surfactant monolayer and therefore decreases the rate of the intermicellar exchange processes,<sup>22–24</sup> but this effect is prone to affect the exchange processes that occur by a fusion–fission mechanism in a region of the micellar interface not connected by the polymer chain.

Another explanation for such a high  $k_w$  value would come from a different interpretation of the  $I_C$  term, considering that it models the quenching reaction in a single water domain in

the cluster but the micelles within do not communicate with each other. Such an interpretation would imply a drastic difference on the model assumed for the structure of polymer-induced clusters. Considering that the polymer chain creates a greater compartmentalization of the aqueous phase and that the quenching process is diffusive, the reduced dimensions of the water domains would facilitate the encounter between the excited probe and the quencher, when both species reside in the same domain at the excitation moment. This was observed by Lianos et al., who studied the interaction of POE with quaternary SDS w/o microemulsions.<sup>27</sup> An increase in the time-dependent quenching rate constant at short times was found, applying a fractal model to their TRFQ results, and it was explained with an increase in the “local” nature of the reaction. By contrast, an increase in microviscosity induced by the polymer presence in the aqueous pseudophase or the possibility of specific interactions of the polymer with the reactants (that could “immobilize” them) was expected to contribute to a decrease of the quenching rate constant.

The fact that the polymer-induced cluster decay component could be well fitted with an integer time dependence shows that the aggregate has a more compact structure than that would be expected from an extended bead necklace, where a fractal dimension should be found.

The assumption that the aggregation number remains practically unchanged in the presence of the polymer is supported by the known stability of the AOT w/o droplets. Brooks and Cates<sup>16</sup> theoretically modeled phase equilibrium in polymer containing microemulsions considering that “polymers combine with droplets without severely affecting their local structure” and found this to be a reasonable assumption, except for very low  $w_0$  values where large departures from experimental results were found. However, the adsorption of the POE at the micellar interface could contribute to an increase in the AOT superficial area, with the polymer acting as a cosurfactant, which would then cause a decrease in the micellar size. This explanation was advanced by Lang et al.<sup>24a</sup> to account for the decrease in the aggregation number of AOT quaternary w/o microemulsions with POE determined by TRFQ with the pair  $\text{Ru}(\text{bpy})_3^{3+}/\text{Fe}(\text{CN})_6^{3-}$ .

A rough idea of the polymer-induced clusters’ size is derived from calculations, based on semidilute athermal scaling theory, of the average number of micelles that compose a cluster. According to Brooks and Cates,<sup>16</sup> the equilibrium number of droplets,  $g_0$ , necessary to solubilize a polymer in the water domain of a microemulsion in the semidilute regime can be estimated from the expression

$$1 + \log(\phi) = -\frac{5}{8\tilde{g}}\left(\frac{g_0}{\tilde{g}}\right)^{-9/4} \quad (18)$$

where  $\phi$  is the volume fraction of polymer-free droplets and  $\tilde{g}$  is a parameter related to the number of micelles necessary to geometrically cover the polymer without increasing the monomer local density and is calculated from

$$\tilde{g} = \frac{l^3}{(4\pi/3)r^3}N^{9/5} \quad (19)$$

In this expression,  $l$  means the monomer length,  $N$  is the degree of polymerization and  $r$  is the droplet radius.

In the present work, the  $g_0$  value obtained is around 22 micelles, which corresponds to a ratio  $g_0/\tilde{g}$  higher than 1 and therefore is not consistent with the assumption of semidilute regime. Besides this, considering that (i) several polymers can

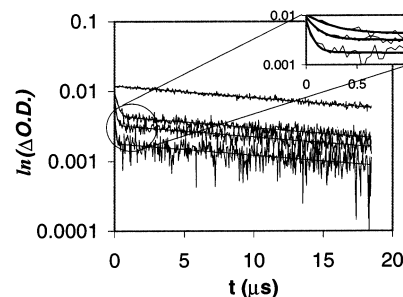


**Figure 8.** Decay curves simulated with expression (17) using:  $\alpha = 0.5$ ;  $k_0 = 3.846 \times 10^4 \text{ s}^{-1}$ ;  $k_0' = 4.000 \times 10^4 \text{ s}^{-1}$ ;  $k_e = 0$ ;  $a_2 = 1$ ;  $k_w = 1.658 \times 10^7 \text{ s}^{-1}$ ;  $n = 0, 0.3015, 0.6030, 1.206$ , and  $n' = 0, 0.2814, 0.5628, 1.126$ —from top to lower curves, respectively.

compose a cluster and (ii) the polymer presence can increase attractive interactions between reversed micelles,<sup>21</sup> larger dimensions should be expected for the clusters. Indeed, the application of the Stokes–Einstein equation to the DLS results of polymer-induced clusters supports this hypothesis. The radius obtained is of the order of several hundred angstroms and therefore five times larger than the radius of an aggregate composed by 22 micelles. Even so, if this  $g_0$  is used to estimate the cluster volume fraction, assuming that one cluster is induced only by one polymer chain, an upper limit of 64% is obtained. This number compares well with the  $\alpha$  parameter obtained from fluorescence quenching with the pair PTSA/ $\text{I}^-$ , indicating that the main contribution to the fluorescence decay, about 70 to 80%, comes from the cluster population. Some care should be taken in the interpretation of these values, since there are other factors influencing the  $\alpha$  parameter such as the emission density of the probe located in the clusters or the partition of this species between the micellar aggregates in the microemulsion. Regarding this last point, it should be noticed that PTSA affinity with POE favors its location in the clusters. In a different set of experiments (not presented), no changes were found in the value of the  $\alpha$  parameter with the variation of the AOT concentration to lower and higher values (keeping the  $w_0$  and POE concentration in the water-pool constant).

The negligible value obtained for the intercept in the logarithm plot of  $(1 - \alpha) \exp(-n)$  vs quencher concentration—see Figure 6b—indicates that  $\alpha$  must be very small in the transient absorption results. Since in this case no specific interaction is expected between the polymer and the probe used, a low  $\alpha$  value could simply reflect a low volume fraction of clusters. This would also explain the invariance of the average aggregation numbers presented in Table 5 for the free reversed micelles in the microemulsions with and without polymer.

Several decays were simulated using expression (17) and a set of constants with values close to the expected ones, except for  $\alpha$ , in which case a value of 0.5 was used for illustration purposes—see Figure 8. It was possible to verify that the faster component decays almost completely within the first micro-seconds, in a time interval that under real conditions would be largely overlapped by the excitation laser signal. The introduction of noise into the calculated decay curves makes the detection of this short component more difficult and the global decay resembles a single exponential, in agreement with the approximations considered in the results section. The increasing contribution of the  $\alpha$  value results in a nonzero intercept for the logarithm plot of the normalized initial decay intensities (not shown). On the other hand, the  $k_0$  values retrieved oscillate with the quencher concentration, probably as a result of using a single exponential to fit an experimental decay with considerable noise. The simulation of decay curves provides some



enlightening concerning the limitations of the method employed and allowed us to test the hypothesis put forward to explain the lack of a polymer effect in the transient absorption data (microsecond range) as opposed to the TRFQ data (nanosecond range).

### Final Comments

Excited-state quenching kinetics applied to AOT microemulsions with hydrophilic polymer POE (MW = 35 000 Da) were studied with transient techniques. Two time scales were investigated using probes with different lifetimes: PTSA for the nanosecond domain and  $\text{Cr}(\text{bpy})_3^{3+}$  for the microsecond domain. The decays obtained were modeled using a bimodal law to account for the two distinct populations of aggregates that compose these microemulsions, polymer-free micelles and polymer-induced clusters, which do not interchange. The decay component corresponding to the population of the latter aggregates was described with a model developed for large percolative clusters with a compact structure. From the nanosecond TRFQ results it was possible to estimate a jump frequency between water-pools of  $10^7 \text{ s}^{-1}$  for the quencher's diffusion within the polymer-induced clusters, which is one to two orders of magnitude higher than the value observed in percolative clusters. This difference was explained considering that the polymer chain, serving as the backbone for the cluster, facilitates the communication between the micelles that compose this aggregate. In the microsecond time scale, it was only possible to estimate the aggregation number for the free reversed micelles that are present in both the systems with and without polymer.

**Acknowledgment.** This work was supported by CQE IV/FCT. P. M. Paulo acknowledges a Ph.D. Grant BD 21698/99 from Praxis XXI. Professor J. M. G. Martinho is acknowledged for the use of the SPC equipment and Dr. A. Federov for performing the measurements. The authors express their gratitude to Professor Mauro Maestri for the generous gift of a sample of  $\text{Cr}(\text{bpy})_3^{3+}$ .

### References and Notes

- (1) Ninham, B. W.; Mitchell, D. J. *J. Chem. Soc., Faraday Trans 2* **1981**, 77, 601.
- (2) Kellay, H.; Binks, B. P.; Hendriks, Y.; Lee, L. T.; Meunier, J. *Adv. Colloid Interface Sci.* **1994**, 49, 85.
- (3) Zulauf, M.; Eicke, H. *J. Phys. Chem.* **1979**, 83 (4), 480.
- (4) Atik, S. S.; Thomas, J. K. *J. Am. Chem. Soc.* **1981**, 103, 3543.
- (5) Jahn, W.; Strey, R. *J. Phys. Chem.* **1988**, 92, 2294.
- (6) Rička, J.; Borkovec, M.; Hofmeier, U. *J. Chem. Phys.* **1991**, 94 (12), 8503.
- (7) Strey, R. *Colloid Polym. Sci.* **1994**, 272, 1005.
- (8) Bardez, E.; Goguillon, B. T.; Keh, E.; Valeur, B. *J. Phys. Chem.* **1984**, 88, 1905.
- (9) Howe, A. M.; McDonald, J. A.; Robinson, B. H. *J. Chem. Soc., Faraday Trans. 1* **1987**, 83, 1007.
- (10) Fletcher, P. D.; Howe, A. M.; Robinson, B. H. *J. Chem. Soc., Faraday Trans. 1* **1987**, 83, 985.
- (11) Fendler, J. H. *Chem. Rev.* **1987**, 87, 877.
- (12) Pileni, M. P.; Huruguen, J. P.; Petit, C. In *The Structure, Dynamics and Equilibrium Properties of Colloidal Systems*; Bloor, D. M., Wyn-Jones, E., Eds.; Kluwer Academic Publishers: The Netherlands, 1990; pp 355–371.
- (13) Huruguen, J. P.; Authier, M.; Greffe, J. L.; Pileni, M. P. *Langmuir* **1991**, 7, 243.
- (14) Cassin, G.; Duda, Y.; Holovko, M.; Badiali, J. P.; Pileni, M. P. *J. Chem. Phys.* **1997**, 107 (7), 2683.
- (15) Kabalnov, A.; Lindman, B.; Olsson, U.; Piculell, L.; Thuresson, K.; Wennerström, H. *Colloid Polym. Sci.* **1996**, 274, 297.
- (16) Brooks, J. T.; Cates, M. E. *Chem. Phys.* **1990**, 149, 97.
- (17) Nagarajan, R. *Langmuir* **1993**, 9, 369.
- (18) Schwuger, M.-J.; Stickdorn, K.; Schomäcker, R. *Chem. Rev.* **1995**, 95, 849.
- (19) Fendler, J. H. *Reversed Micellar Systems* **1976**, 9, 153.
- (20) Lusvardi, K. M.; Schubert, K.-V.; Kaler, E. W. *Ber. Bunsen-Ges. Phys. Chem.* **1996**, 100 (3), 373.
- (21) Laia, C. A. T.; Brown, W.; Almgren, M.; Costa, S. M. B. *Langmuir* **2000**, 16, 465.
- (22) Meier, W. *Langmuir* **1996**, 12, 1188.
- (23) Meier, W. *J. Phys. Chem. B* **1997**, 101, 919.
- (24) (a) Suarez, M. J.; Levy, H.; Lang, J. *J. Phys. Chem.* **1993**, 97, 9808. (b) Suarez, M. J.; Lang, J. *J. Phys. Chem.* **1995**, 99, 4626. (c) Lianos, P. *J. Phys. Chem.* **1996**, 100, 5155. (d) Lang, J. *J. Phys. Chem.* **1996**, 100, 5156.
- (25) Hasegawa, M.; Yamasaki, Y.; Sonta, N.; Shindo, Y.; Sugimura, T.; Kitahara, A. *J. Phys. Chem.* **1996**, 100, 15575.
- (26) Bohne, C.; Abuin, E. B.; Scaiano, J. C. *Langmuir* **1992**, 8, 469.
- (27) (a) Lianos, P.; Modes, S.; Staikos, G.; Brown, W. *Langmuir* **1992**, 8, 1054. (b) Papoutsis, D.; Lianos, P.; Brown, W. *Langmuir* **1993**, 9, 663. (c) Papoutsis, D.; Lianos, P.; Brown, W. *Langmuir* **1994**, 10, 3402.
- (28) Alexandridis, P.; Holzwarth, J. F.; Hatton, T. A. *J. Phys. Chem.* **1995**, 99, 8222.
- (29) Tingey, J. M.; Fulton, J. L.; Smith, R. D. *J. Phys. Chem.* **1990**, 94, 1997.
- (30) Mays, H.; Ilgenfritz, G. *J. Chem. Soc., Faraday Trans.* **1996**, 92 (17), 3145.
- (31) Koper, G. J.; Sager, W. F.; Smeets, J.; Bedeaux, D. *J. Phys. Chem.* **1995**, 99, 13291.
- (32) Laia, C. A. T.; López-Cornejo, P.; Costa, S. M. B.; d'Oliveira, J.; Martinho, J. M. G. *Langmuir* **1998**, 14, 3531.
- (33) Laia, C. A. T.; Brown, W.; Almgren, M.; Costa, S. M. B. *Langmuir* **2000**, 16, 8763.
- (34) Jóhannsson, R.; Almgren, M.; Alsins, J. *J. Phys. Chem.* **1991**, 95, 3819.
- (35) Almgren, M.; Jóhannsson, R. *J. Phys. Chem.* **1992**, 96, 9512, and references therein.
- (36) Jóhannsson, R.; Almgren, M. *Langmuir* **1993**, 9, 2879.
- (37) Infelta, P. P.; Grätzel, M.; Thomas, J. K. *J. Phys. Chem.* **1974**, 78 (2), 190.
- (38) Tachiya, M. *Chem. Phys. Lett.* **1975**, 33 (2), 289.
- (39) Almgren, M.; Jóhannsson, R.; Eriksson, J. C. *J. Phys. Chem.* **1993**, 97, 8590.
- (40) Salazar, F. A.; Federov, A.; Berberan-Santos, M. N. *Chem. Phys. Lett.* **1997**, 271, 361.
- (41) Press, W. H.; Teukolsky, S. A.; Vetterling, W. T.; Flannery, B. P. *Numerical Recipes in FORTRAN, The art of Scientific Computing*, 2nd ed.; Cambridge University Press: New York, 1992.
- (42) O'Connor, D. V.; Phillips, D. *Time-Related Single Photon Counting*; Academic Press: London, 1984.
- (43) Togashi, D. M.; Costa, S. M. B. *Phys. Chem. Chem. Phys.* **2000**, 2, 5437.
- (44) Lang, J. In *The Structure, Dynamics, and Equilibrium Properties of Colloidal Systems*; Bloor, D. M., Wyn-Jones, E., Eds.; Kluwer Academic Publishers: The Netherlands, 1990; pp 1–38.
- (45) (a) Miller, D. D.; Evans, D. F. *J. Phys. Chem.* **1989**, 93, 323. (b) Miller, D. D.; Magid, L. J.; Evans, D. F. *J. Phys. Chem.* **1990**, 94, 5921.
- (46) Verbeeck, A.; De Schryver, F. C. *Langmuir* **1987**, 3, 494.
- (47) Maestri, M.; Bolleta, F.; Moggi, L.; Balzani, V.; Henry, M. S.; Hoffman, M. Z. *J. Am. Chem. Soc.* **1978**, 100 (9), 2694.
- (48) Serpone, N.; Jamieson, M. A.; Henry, M. S.; Hoffman, M. Z.; Bolleta, F.; Maestri, M. *J. Am. Chem. Soc.* **1979**, 101 (11), 2907.